Received: 21 February 2022 | Revised: 25 June 2022 | Accepted: 1 July 2022

DOI: 10.1002/pld3.429

ORIGINAL RESEARCH

American Society of Plant Biologists | SEB | WILEY

The Arabidopsis T-DNA mutant SALK_008491 carries a 14-kb deletion on chromosome 3 that provides rare insights into the plant response to dynamic light stress

Laura S. Lopez[1] | Carsten Völkner[1,2] | Philip M. Day[1] | Chance M. Lewis[1] | Chase L. Lewis[1] | Dominik Schneider[3] | Viviana Correa Galvis[4] | Jeffrey A. Cruz[5,6] | Ute Armbruster[4] | David M. Kramer[5,6] | Hans-Henning Kunz[1,2]

[1]School of Biological Sciences, Washington State University, Pullman, Washington

[2]Department of Plant Biochemistry, LMU Munich, Planegg-Martinsried, Germany

[3]Compact Plants Phenomics Center, Washington State University, Pullman, Washington, USA

[4]Max Planck Institute of Molecular Plant Physiology, Potsdam, Germany

[5]Department of Biochemistry and Molecular Biology, Michigan State University, East Lansing, Michigan, USA

[6]Department of Energy Plant Research Laboratory, Michigan State University, East Lansing, Michigan, USA

Correspondence
Hans-Henning Kunz, School of Biological Sciences, Washington State University, PO Box 644236, Pullman, WA 99164-4236, USA.
Email: henning.kunz@wsu.edu

Funding information
H.-H. K., D. M. K., and U. A. were funded by the 3rd call ERA-CAPS grant (National Science Foundation [NSF] IOS-1847382, NSF IOS-1847193, and Deutsche Forschungsgemeinschaft [DFG] AR 808/4-1, respectively). H.-H. K. also received funding from an NSF Career Award (IOS-1553506) and the DFG (SFB-TR 175, project B09). Plant phenotyping was realized through an M.J. Murdock Charitable Trust (MJMCT) equipment grant (No. SR-2016049) to H.-H. K. DEPI phenotyping and data analyses tools

Abstract

In nature, plants experience rapid changes in light intensity and quality throughout the day. To maximize growth, they have established molecular mechanisms to optimize photosynthetic output while protecting components of the light-dependent reaction and CO_2 fixation pathways. Plant phenotyping of mutant collections has become a powerful tool to unveil the genetic loci involved in environmental acclimation. Here, we describe the phenotyping of the transfer-DNA (T-DNA) insertion mutant line SALK_008491, previously known as *nhd1-1*. Growth in a fluctuating light regime caused a loss in growth rate accompanied by a spike in photosystem (PS) II damage and increased non-photochemical quenching (NPQ). Interestingly, an independent *nhd1* null allele did not recapitulate the NPQ phenotype. Through bulk sequencing of a backcrossed segregating F_2 pool, we identified an ~14-kb large deletion on chromosome 3 (Chr3) in SALK_008491 affecting five genes upstream of *NHD1*. Besides *NHD1*, which encodes for a putative plastid Na^+/H^+ antiporter, the stromal NAD-dependent D-3-phosphoglycerate dehydrogenase 3 (*PGDH3*) locus was eradicated. Although some changes in the SALK_008491 mutant's photosynthesis can be assigned to the loss of PGDH3, our follow-up studies employing respective single mutants and complementation with overlapping transformation-competent artificial chromosome (TAC) vectors reveal that the exacerbated fluctuating light sensitivity in SALK_008491 mutants result from the simultaneous loss of PGDH3 and NHD1. Altogether, the data obtained from this large deletion-carrying mutant provide new and unintuitive insights into the molecular mechanisms that function to protect the photosynthetic machinery. Moreover, our study renews calls for caution when setting up reverse genetic studies using T-DNA lines. Although second-site

were supported by the U.S. Department of Energy (DOE) Office of Science, Basic Energy Sciences, under Awards DEFG02-91ER20021 and DE-SC0007101 to D. M. K.

insertions, indels, and SNPs have been reported before, large deletion surrounding the insertion site causes yet another problem. Nevertheless, as shown through this research, such unpredictable genetic events following T-DNA mutagenesis can provide unintuitive insights that allow for understanding complex phenomena such as the plant acclimation to dynamic high light stress.

KEYWORDS
chloroplast, forward genetics, phenotyping, photosynthesis, redox poise, T-DNA insertion mutants

1 | INTRODUCTION

Under field conditions, land plants are constantly exposed to changing environmental triggers such as shifts in light, temperature, and water availability. They have evolved a myriad of molecular mechanisms that aid in rapid acclimation to the challenges to maximize their growth potential (Armbruster et al., 2017). Interestingly, much of the sensing and initial response takes place in chloroplasts. A detailed understanding of these pathways and their genetic components may have great potential to engineer the so-called green hub with the goal to design more tolerant plants with faster acclimation capabilities (Kleine et al., 2021).

Plant phenotyping of mutant collections, for example, by tracking photosynthesis via chlorophyll fluorescence as a proxy for plant performance, has become a hallmark to identify genetic loci that aid in light acclimation (Cruz et al., 2016). Sudden spikes and drops in light intensities are challenging for the photosynthetic machinery. If the surplus of incoming light energy cannot be effectively dealt with, both photosystems (PSs), but especially PSII, are prone to photodamage. Although PSII damage, differently from PSI photoinhibition, can be repaired quickly, plants employ several strategies to avoid this unnecessary burden: (1) the main component of non-photochemical quenching (NPQ), qE, quenches incoming light energy through heat dissipation; (2) photosynthetic control, that is, slowing down linear electron flow (LEF) between PSII and PSI via the Cytb6f complex, is critical to protect PSI; and (3) cyclic electron flow (CEF) between Cytb6f and PSI plays an important role to protect and/or mitigate PSI damage by avoiding PSI acceptor side limitation, which originates from a sudden drop in Calvin–Benson–Bassham (CBB) cycle activity and concomitant overreduction of the stroma (Kramer & Kunz, 2021). All three described protective mechanisms are linked to the H^+ gradient (ΔpH) established across the thylakoid membrane after the onset of illumination (Armbruster et al., 2017). ΔpH is one component of the proton motif force (pmf) driving the ATP synthase. The second pmf component is the membrane potential $\Delta\psi$. Their relative quantitative contribution (pmf partitioning) remains under debate (Johnson & Ruban, 2013). Nevertheless, it varies depending on the light conditions that have implications for all aforementioned strategies. Because overprotection diminishes photosynthesis output, plants can rapidly adjust pmf partitioning to turn off protection when light intensity drops. This is primarily achieved via activity of H^+-coupled ion transporters and ion channels in the thylakoid membrane (Armbruster et al., 2017). NPQ can be easily determined through changes in PSII chlorophyll fluorescence. Therefore, the method has been employed in many studies to characterize the consequences in gene loss or gain of function mutants affected in loci encoding for thylakoid ion transport proteins (Cruz et al., 2016; Höhner et al., 2019; Li et al., 2021).

The majority of Arabidopsis mutants studied by plant scientists are publicly available transfer-DNA (T-DNA) insertion lines. Over the last years, it has become clear that many T-DNA lines carry second-site insertions and deletions of varying degree and sizes (Dash et al., 2021; OMalley et al., 2015). Even complex genome reorganizations have been reported (Jupe et al., 2019). Mutant genome sequencing has become very affordable and is strongly advised especially in cases where independent alleles are not available. Notably, unanticipated second-site insertions have provided a slew of loss-of-function mutants even in loci that lacked mapped insertions previously (Höhner et al., 2019). Therefore, the genome coverage of the publicly available T-DNA mutants is much higher than initially expected, which is encouraging for scientists interested in using T-DNA populations for forward genetic screens.

In this study, we describe the discovery of previously unknown 14-kb genomic deletion on chromosome 3 (Chr3) in the mutant line SALK_008491. The deletion comprises six loci in total. Interestingly, two of the six genes encode for plastid proteins. In combination, their loss is responsible for a previously unknown severe sensitivity to fluctuating light. Our finding was made possible through automated plant phenotyping and insertion mapping of bulk mutant genome sequencing data.

2 | RESULTS

2.1 | Automated phenotyping on previously published plastid ion transport mutant reveals several alternating parameters in SALK_008491 from wild type

In an earlier study, we reported on the specific and highly reproducible growth light-dependent NPQ changes in Arabidopsis mutants defective in plastid ion transport proteins (Höhner et al., 2019). To

expand on our earlier datasets, we reran a fluctuating light experiment but included the insertion line SALK_008491, previously published as *nhd1-1* (Muller et al., 2014). Specifically, we were interested in this line because of the ongoing uncertainty if the transporter NHD1 (At3g19490) localizes to the plastid inner envelope and or the thylakoid membrane (Tomizioli et al., 2014).

Fourteen-day-old Arabidopsis plants grown under 12/12-h light–dark regimes (120 µmol photons m^{-2} s^{-1}) were transferred into the phenotyping unit, and a variety of growth parameters were monitored for 20 days. Initially, the growth rate was identical among genotypes (Figure 1a,b), similar to F_v/F_m values (max quantum efficiency of PSII, Figure 1c,d). Interestingly, PSII efficiency (ΦPSII) was lower in SALK_008491, whereas steady-state NPQ was above wild-type (WT) level throughout the entire experiment (Figure 1e–h). After 1 week, the growth regime was switched from continuous light to dynamic light conditions (12/12 h, 1 min

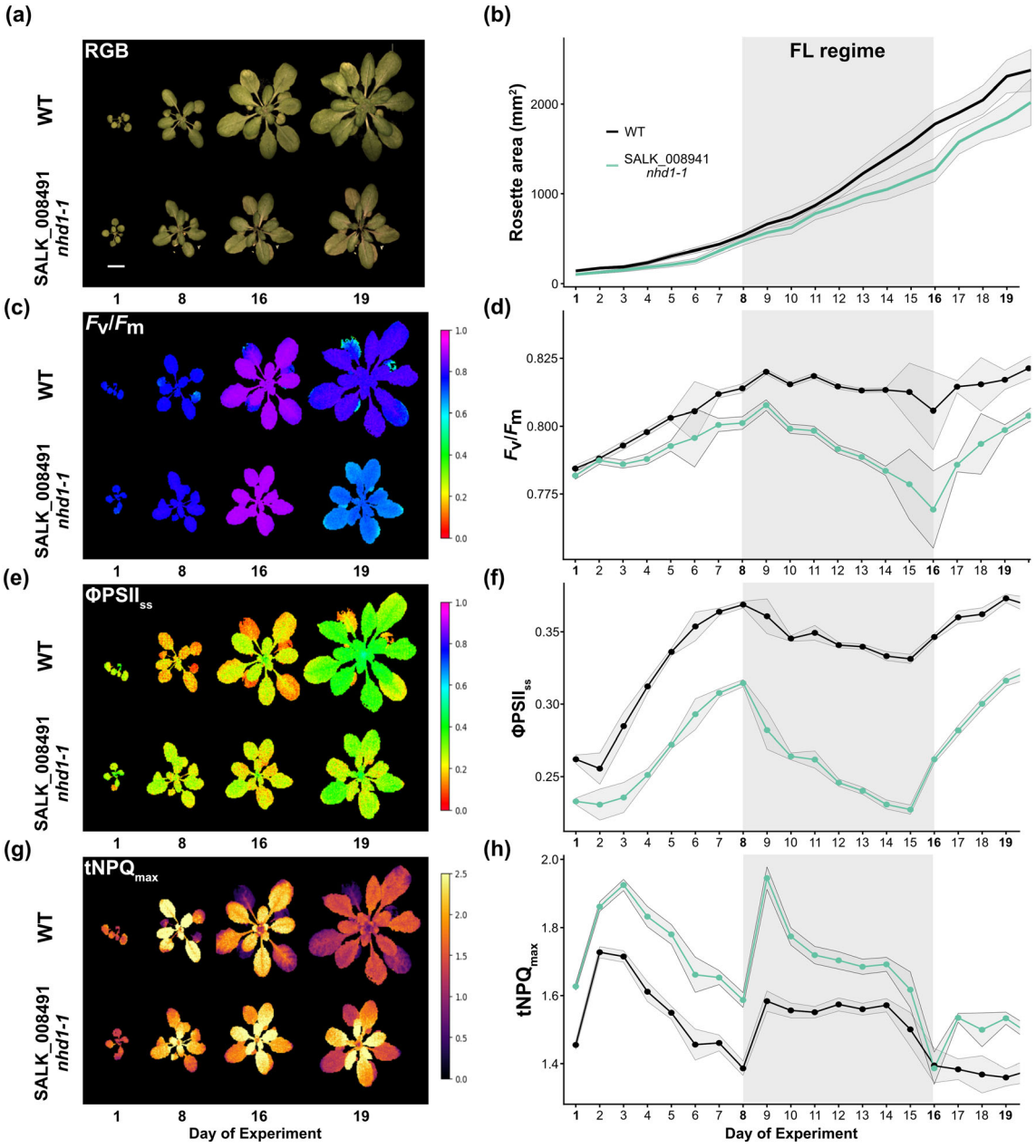

FIGURE 1 Automated phenotyping of WT and SALK_008491, formerly known as *nhd1-1*. Fourteen-day-old plants were transferred into LemnaTech phenotyping unit. Parameters were continuously monitored. For the first 7 days, plants were subjected to control light conditions (100 µmol photons m^{-2} s^{-1} in a 12-h light/12-h dark cycle at 22°C). From Day 8 until Day 16 (gray area), plants were subjected to a fluctuating light (FL) regime, which included an additional 1 min at 500 µmol photons m^{-2} s^{-1} every 5 min. RGB images (a) and PAM measurements (c, e, g) were acquired daily and used for plots in (b), (d), (f) (steady-state ΦPSII, average of the last two induction curve values), and (h) (maximum transient NPQ, average of the last two induction curve values). Data are presented as mean ± SEM ($n = 19$).

500 µmol photons m^{-2} s^{-1}, 4 min 100 µmol photons m^{-2} s^{-1}) because exacerbated phenotypes have been reported for several thylakoid ion transport-deficient mutants exposed to dynamic growth light (Li et al., 2021). Indeed, SALK_008491 plants responded differently from WT plants. The previously observed differences in steady-state NPQ and ΦPSII became more pronounced. Additionally, PSII damage, represented by a significant drop of F_v/F_m in SALK_008491, was noticeable. This defect was accompanied by a reduction in growth rate, measured by the observed increases in leaf areas. SALK_008491 mutant plants were visually smaller. After 1 week of dynamic light treatment, the growth light conditions were returned to continuous light (12/12 h, 120 µmol photons m^{-2} s^{-1}). Subsequently, SALK_008491 recovered but continued to exhibit the same differences in NPQ

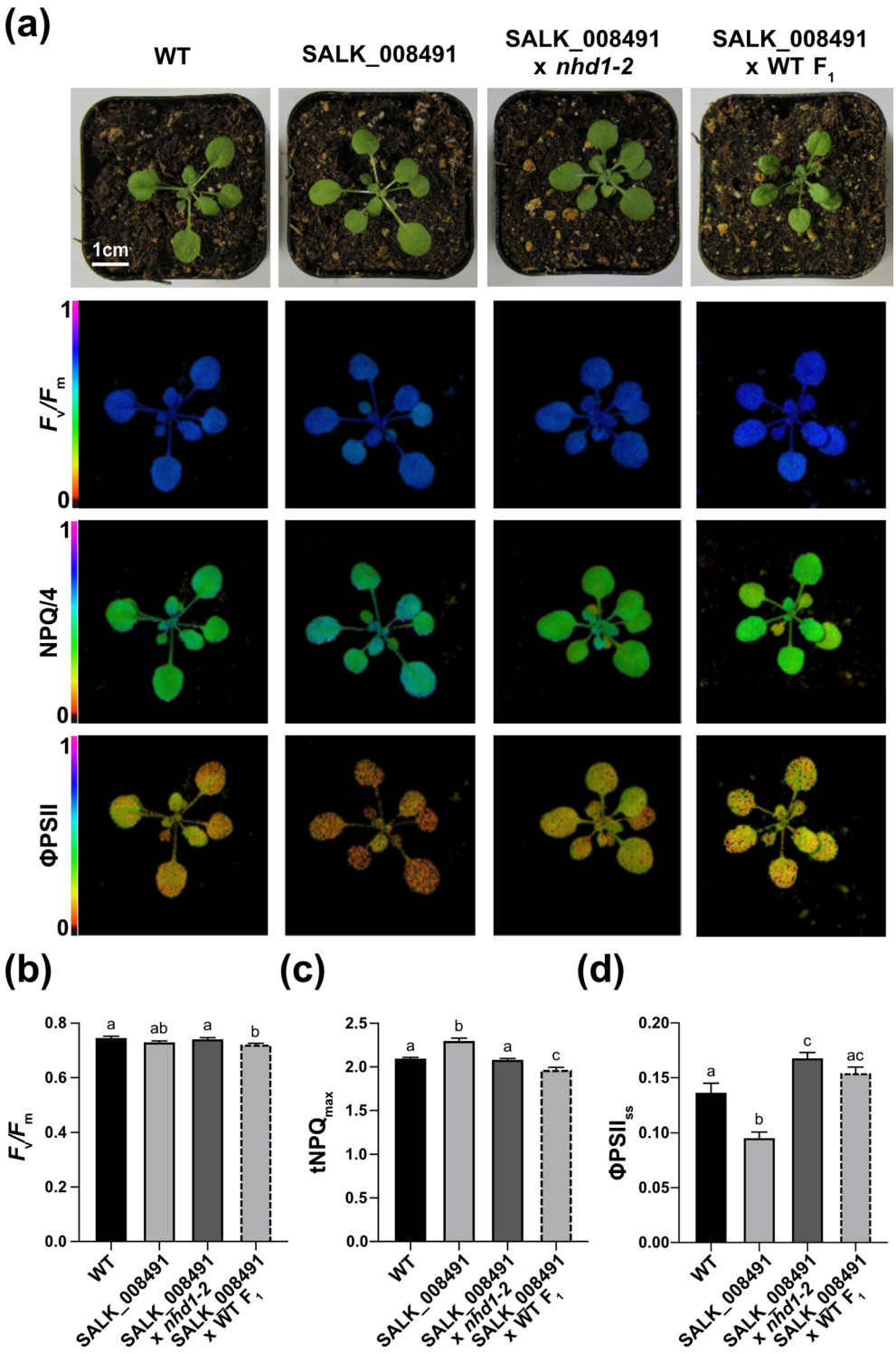

FIGURE 2 Loss of NHD1 does not result in elevated NPQ when grown under control light. (a) Twenty-eight-day-old mutants grown under control light conditions at 90 µmol photons m^{-2} s^{-1} appear undistinguishable from the WT. False color images demonstrate that SALK_008491 is the only line with elevated NPQ levels and lower ΦPSII levels compared with WT, SALK_008491x*nhd1-2* cross (*nhd1-1nhd1-2*), and SALK_008491xWT (backcross SALK_008491xWT). Statistical analysis of F_v/F_m (b), $tNPQ_{max}$ (c), and $\Phi PSII_{ss}$ (d). Data are shown as mean ± SEM ($n = 3$). Different letters indicate different levels of significance ($p < .05$) as determined by one-way ANOVA and Tukey's multiple comparisons test.

and ΦPSII from WT as recorded during the first growth phase under continuous light (experimental days: 1–7).

2.2 | Transient high NPQ in SALK_008491 is caused by recessive gene loss other than NHD1

Initially, we were interested to test if the increase in steady-state NPQ discovered in SALK_008491 was linked to the suggested function of NHD1 as a Na^+/H^+ antiporter (Furumoto et al., 2011; Muller et al., 2014). Therefore, we crossed it with the *nhd1-2* allele, which is homozygous lethal due to an unknown second-site insertion (Muller et al., 2014). In addition, we also backcrossed SALK_008491 into the WT (Figure 2a). Subsequently, we grew up the resulting F_1 individuals in 12/12-h light–dark regime (at continuous light: 120 μmol photons m^{-2} s^{-1}) and determined chlorophyll fluorescence parameters (Figure 2a–d). Surprisingly, the F_1 backcrosses with *nhd1-2* but also with WT did not show any NPQ changes (Figure 2c). This meant that the high NPQ trait in the mutant is recessive but also that elevated NPQ found in SALK_008491 is unlikely related to a loss of NHD1 function.

Therefore, the F_2 progeny population from the SALK_008491 to WT backcross was grown at 12/12-h light–dark regime (at continuous light: 120 μmol photons m^{-2} s^{-1}) and scored for 21-day-old individuals with higher NPQ (Figure 3a). The segregation ratio was roughly 1:3 (22 individuals with high NPQ vs. 68 individuals with WT-like NPQ), that is, typical Mendelian segregation of a single genetic locus as causative for the phenotype.

Next up, we collected equal tissue amounts from all mutant individuals with high NPQ into one pool and isolated genomic DNA (gDNA). To determine the exact molecular cause of the phenotype, we used Illumina-based genome resequencing of our gDNA pool. We aligned all reads to the *Arabidopsis thaliana* genome (Col-0 accession) and compared it with sequencing reads obtained from a WT control (Figure 3b). Just upstream of the originally annotated T-DNA insertion site on Chr3 in SALK_008491, we discovered a 14-kb deletion (Chr3 6,741,088–6,755,390, Figure S1a) in total affecting six annotated genes (At3g14940–At3g19490, Table 1) including *NHD1*. Subsequently, PCR-based genotyping

TABLE 1 Identified disrupted loci in SALK_008491 and respective functional annotations

Locus	Molecular function according to TAIR10	SUBA—subcellular protein location
At3G19440	Pseudouridine synthase family protein	Mitochondrion
At3G19450	ATCAD4, cinnamyl alcohol dehydrogenase 4	Cytosol
At3G19460	ER-associated membrane protein of unknown function	Plasma membrane
At3G19470	F-box and associated interaction domains-containing protein	Cytosol
At3G19480	PGDH3 involved in the plastid phosphorylated pathway of serine biosynthesis	Plastid
At3G19490	NHD1 associated as a Na^+/H^+ antiporter that extrudes sodium in exchange for protons	Plastid

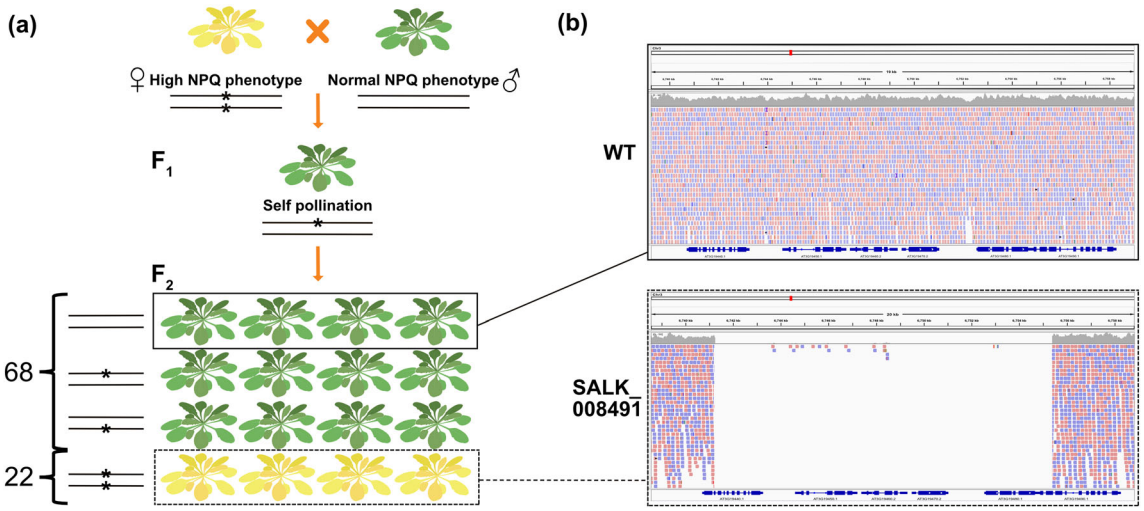

FIGURE 3 Backcrossing of SALK_008491 into the WT and identification of a large deletion in the F_2 bulk sequencing population (a). The T-DNA insertion line SALK_008491 with elevated NPQ levels was backcrossed to WT (normal NPQ levels). The F_1 generation self-pollinated to obtain an F_2 population. Ninety F_2 individuals were potted and screened for high NPQ levels: 68 individuals had normal and 22 individuals elevated NPQ levels, resulting in a segregation ratio of ~3:1. (b) IGV image of the sequencing reads of SALK_008491 gDNA aligned to the published *Arabidopsis thaliana* genome (TAIR10) revealed a 14-kb gap in which the genes are entirely or partially deleted (At3g19440–At3g19490).

confirmed the absence of all six loci and the position of the T-DNA insertion (Figure S1a,b).

2.3 | Transient high NPQ in SALK_008491 is caused by loss of PGDH3

Within the 14-kb deletion, we identified the plastid stromal enzyme PHOSPHOGLYCERATE DEHYDROGENASE 3 (PGDH3) encoded by locus *At3g19480*. PGDH3 is one of three PGDH isoforms in Arabidopsis to function in the phosphoserine pathway (Benstein et al., 2013). Previous studies have shown that isoform PGDH3 is important for full photosynthetic capacity in *A. thaliana* (Casatejada-Anchel et al., 2021; Hohner et al., 2021). Besides changes in CO_2 fixation, the loss of *PGDH3* results in a characteristic increase in transient NPQ ($tNPQ_{max}$) at non-saturating light conditions (Hohner et al., 2021).

Therefore, we employed previously described T-DNA insertion mutants *pgdh3-1* and *pgdh3-2* (Toujani et al., 2013) to create F_1 generation crosses with SALK_008491. As controls, we also generated F_1 backcrosses with WT. The entire plant panel was grown up in a 12/12-h light–dark regime (at continuous light: 120 µmol photons m^{-2} s^{-1}) and at a plant age of 21 days assayed for transient NPQ during photosynthesis induction at growth light (Figure 4a,b). All backcrosses to WT showed no significant NPQ difference to the WT, whereas NPQ in F_1 SALK_008491 × *pgdh3* plants resembled *pgdh3-1* and *pgdh3-2* single-mutant lines. We followed up with immunoblotting and enzyme activity assays of total leaf extracts. Indeed, leaf PGDH protein level and total PGDH activity in SALK_008491 did not deviate from *pgdh3-1* and *pgdh3-2*, that is, were reduced by 40–50% compared with WT (Figure S2a,b). In addition, SALK_008491 showed absence of NHD1 protein in leaves. Transforming SALK_008491 with a *pUBQ10::PGDH3-RFP* construct restored PGDH3 enzyme amount and total PGDH activity, along

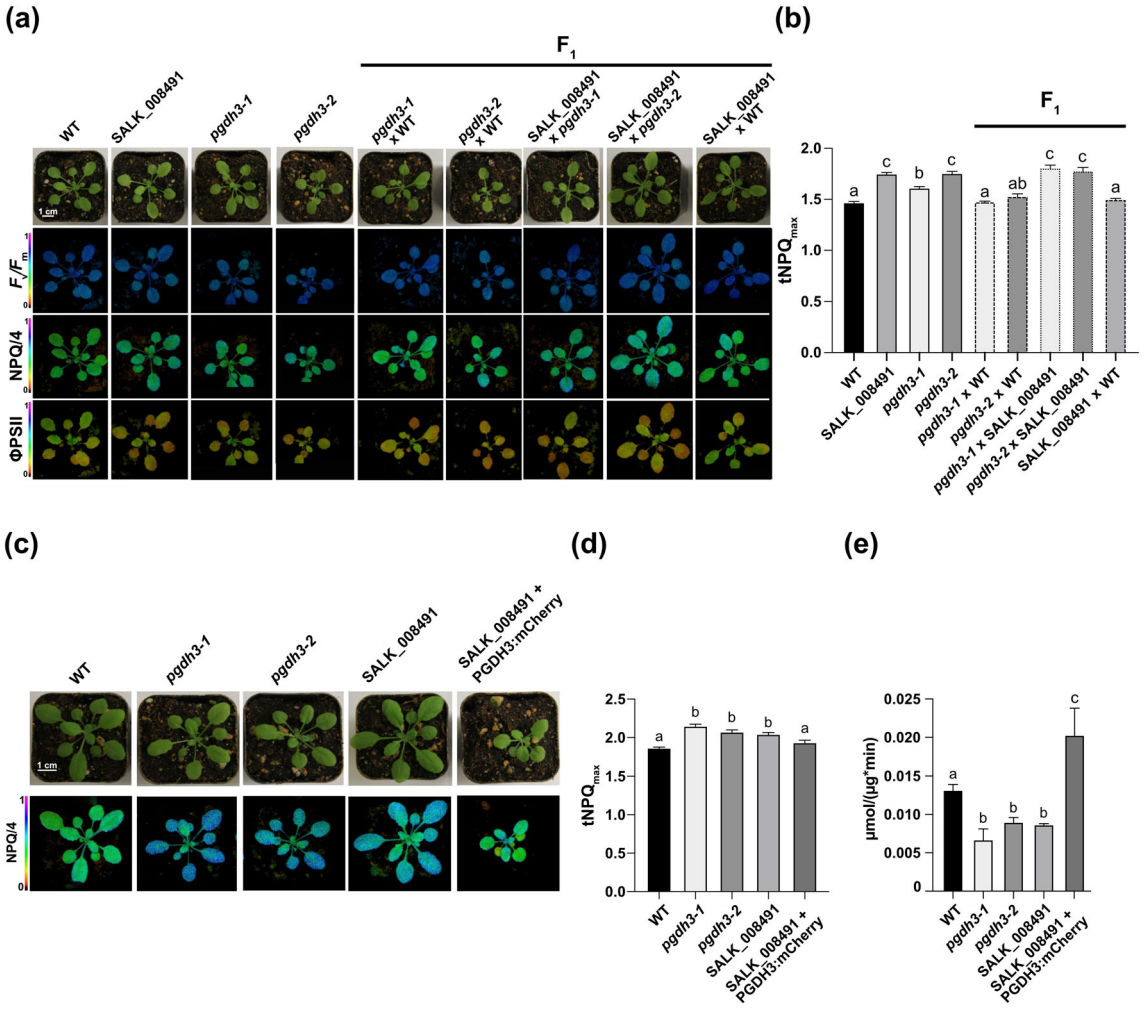

FIGURE 4 Loss of PGDH3 is causative for elevated transient NPQ. (a, b) Allelism test demonstrates that high NPQ levels are caused by the loss of PGDH3, as seen in SALK_008491, SALK_008491x*pgdh3-1*, SALK_008491x*pgdh3-2*, *pgdh3-1*, and *pgdh3-2*. Backcrossing into the WT restored NPQ. Data in (b) are presented as mean ± SEM ($n = 3$). SALK_008491 transformed with a *pUBQ10::PGDH3-mCherry* shows WT-like NPQ levels (c, d) and recovered enzyme activity (e) (mean ± SEM, $n = 4$). Different letters denote different levels of significance ($p < .05$) as determined by one-way ANOVA and Tukey's multiple comparisons test.

with transient NPQ, which was now indistinguishable from WT (Figure 4c–e).

In summary, our results indicate that the recorded changes in NPQ dynamics in SALK_008491 are mostly unrelated to a loss of putative plastid Na^+/H^+ antiporter NHD1 but rather originate from the lack of PGDH3 activity due to the loss of the entire locus within the deletion.

2.4 | Dynamic environmental photosynthetic imaging reveals additional changes in photosynthesis specific to SALK_008491

We were curious if the loss of six genes is only affecting plant performance via the loss of *PGDH3*. Therefore, we ran a dynamic environmental photosynthetic imaging (DEPI) experiment (Cruz et al., 2016). This allowed monitoring of more plant individuals from all genotypes side by side. Additionally, we were able to use higher light intensities, simulate "sinusoidal" illumination (peaking at 500 μmol photons m^{-2} s^{-1}; Day 2), and a combination of "fluctuating" and "sinusoidal" light peaking at 1000 μmol photons m^{-2} s^{-1} (Days 3 and 5, Figure 5a). Although the DEPI system identified lower ΦPSII specifically in SALK_008491, changes in NPQ, qE, and qI (photoinhibition) from WT were barely detectable in any genotype if constant growth light was applied (Days 1 and 4, Figure 5b–e). This changed when the light intensity was ramped up towards the middle of the day (Day 2). NPQ and its main component qE increased drastically in all three mutant lines. Again, SALK_008491 revealed a more pronounced loss of ΦPSII compared with single *pgdh3* loss-of-function lines. Although the three genotypes responded similarly to the first fluctuating light treatment (Day 3), their behavior diverged when the fluctuating light treatment was repeated on Day 5. Here, SALK_008491 maintained high NPQ and qE, whereas both *pgdh3* loss-of-function lines did not follow the same trend (Figure 5c,d). The overall impression of the DEPI experiment was that the sinusoidal growth light on Day 2 triggered the most extreme differences between the mutant and WT plants.

To dissect the effects recorded in SALK_008491, *pgdh3-1*, and *pgdh3-2* from a different perspective, we plotted the dependence of qE against LEF for all data points collected on Days 1–3 (Figure 5f). This approach was previously described to estimate the "qE sensitivity" of the system, likely reflecting factors that modulate the relationship between electron flux and lumen acidification, which controls the extent of qE (Kanazawa & Kramer, 2002). An increase in this relationship could reflect activation of CEF, the downregulation of the chloroplast ATP synthase (limiting proton efflux from the lumen), or changes in the partitioning of pmf into ΔpH or $\Delta\psi$ (Strand & Kramer, 2014). Although the independent *pgdh3* loss-of-function mutants showed similar but homogenous variations from WT, SALK_008491 behaved more extreme with higher qE values seen at lower rates of LEF.

In summary, the DEPI data reveal that SALK_008491 shares several phenotypic features with *pgdh3* mutant lines. Importantly, it also exhibits additional phenotypic traits that could be unrelated or conditional to the effects caused by a *PGDH3* loss. This may hint at a previously undocumented role in photosynthesis or chloroplast function of one of the five other genes lost through the deletion in SALK_008491.

2.5 | The conditional gene loss of PGDH3 and NHD1 makes SALK_008491 highly susceptible to dynamic high light stress

In our initial phenotyping experiment (Figure 1), SALK_008491 plants showed decreased growth rates in response to fluctuating light. To dissect this behavior, 14-day-old plants (12/12 h, continuous light 120 μmol photons m^{-2} s^{-1}) were exposed to a long-term fluctuating light treatment (12/12 h; 1 min 900 μmol photons m^{-2} s^{-1}, 4 min 90 μmol photons m^{-2} s^{-1}) (Schneider et al., 2019). After 2 weeks of treatment, we determined photosynthetic parameters and above-ground biomass (Figure 6a–c and Movie S1). Among all genotypes in the experiment, SALK_008491 responded most dramatically with strong photodamage represented by low F_v/F_m values most apparent in older leaves. NPQ levels in SALK_008491 were still above the WT, but this was restricted to the less severely affected young tissue. SALK_008491 showed very poor overall growth compared with all controls (Figure 6c). All light stress-induced damages recovered within 2 days after switching the growth light to 12/12 h, continuous light 120 μmol photons m^{-2} s^{-1} (Movie S2). According to F_1 WT backcrosses, the extreme fluctuating growth light sensitivity was due to a recessive genetic effect (Figure S3a). F_v/F_m in SALK_008491 did not differ from WT if constant high light stress was applied (Figure S3b).

We also investigated *pgdh3* and *nhd1* single mutants. In line with earlier studies, loss of *PGDH3* also resulted in PSII damage. Transient NPQ remained higher and ΦPSII lower than WT. All effects were less severe than in SALK_008491. Interestingly, we also observed clear changes from WT in *nhd1-1nhd1-2* plants under fluctuating light. Specifically, old leaves exhibited low F_v/F_m and ΦPSII values, whereas NPQ was similar to WT. None of the single mutants in the other four deleted loci on Chr3 in SALK_008491 exhibited any light stress sensitivity (Figure S3c,d). We transformed SALK_008491 with two different but overlapping transformation-competent artificial chromosome (TAC) clones (K19N23 and K25N10) (Liu et al., 1999). Both include the *PGDH3* and *NHD1* loci. However, although K19N23 harbors all six genes affected by the deletion in SALK_008491, TAC clone K25N10 only encodes *PGDH3*, *NHD1*, and loci downstream of *NHD1* (Figure S4). Both clones complemented the fluctuating light stress sensitivity observed in SALK_008491 and showed recovered F_v/F_m and fresh weight (Figure 6a–c).

In summary, our results indicate a previously unknown role for NHD1 in the plant response to dynamic light stress. More importantly, the extreme sensitivity towards these growth conditions as observed in large deletion line SALK_008491 seems to be an additive effect due to the absence of two nuclear encoded plastid proteins PGDH3 and NHD1.

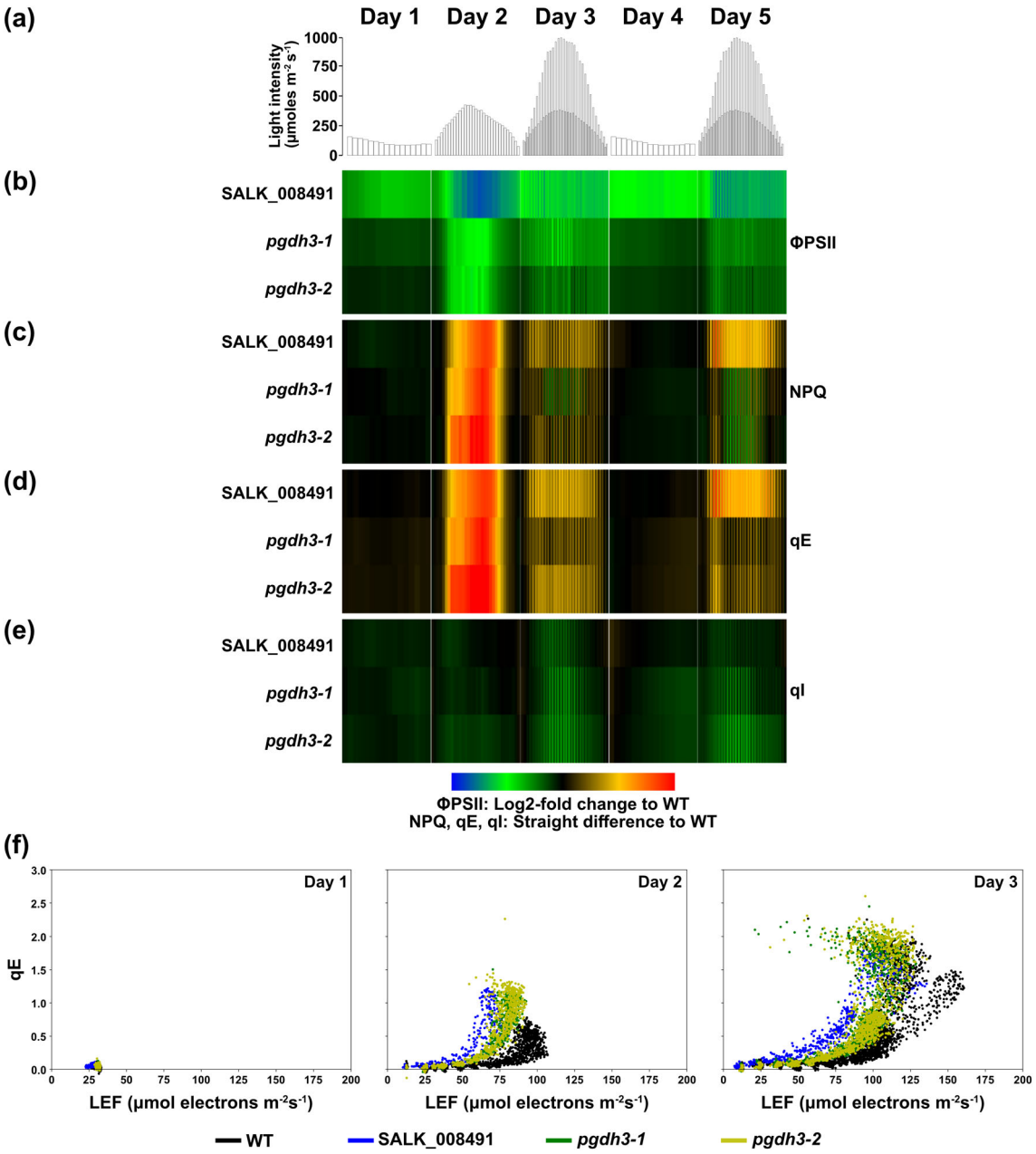

FIGURE 5 DEPI phenotyping platform reveals differences between SALK_008491 and *pgdh3* loss-of-function alleles. Twenty-one-day-old plants were moved to the DEPI chamber and treated with light regimes indicated in (a). Data are presented as change from WT, with ΦPSII (b) being presented as $\log_2$-fold change (ranging from −0.3 to 0.3), whereas NPQ (c), qE (d), and qI (e) are indicated as straight difference (ranging from −0.6 to 0.6). The different approaches to comparing results (log fold vs. differences) are related to differences in the types of parameters measured. ΦPSII estimates yield (the fraction of light energy being used for photochemistry), and thus, a twofold change would have similar magnitude effects. On the other hand, the NPQ components are related to the scalar concentrations of quenchers (Holzwarth et al., 2013), which have nonlinear effects on the yield photochemistry. In this case, under very low light, the WT may have NPQ that is nearly zero, so that comparing with a plant exhibiting even small increases in NPQ (which have only minor effects on photochemical efficiency) would result in extremely large ratios or log-fold changes. (f) qE dependence on linear electron flow (LEF) for each time point measured on Days 1–3 and their respective light regimes.

3 | DISCUSSION

Initial phenotyping experiments revealed unreported changes in photosynthesis and growth behavior of SALK_008491 T-DNA insertion mutants. These changes were exacerbated under dynamic growth light conditions. SALK_008491 had been previously published as *nhd1-1*, that is, lacking the plastid Na^+/H^+ exchanger NHD1 (Muller et al., 2014).

FIGURE 6 Simultaneous loss of *NHD1* and *PGDH3* renders SALK_008491 highly susceptible to fluctuating high light stress. (a) Fourteen-day-old SALK_008491, WT, and single-mutant controls were subjected to fluctuating light treatment and imaged after 2 weeks. Although *pgdh3-1* and *nhd1-1nhd1-2* show some degree of light stress susceptibility, this was much more pronounced in SALK_008491. Transformation with overlapping TAC clones (both carry *NHD1* and *PGDH3* loci) restored WT behavior in SALK_008491 + $_{TAC}$*K25N10* and SALK_008491 + $_{TAC}$*K19N23* plants exposed to fluctuating high light. (c) Plot of F_v/F_m values from PAM measurements in (a) and (b) and fresh weights of plants (d). Bar graphs are presented as mean ± SEM ($n = 3$). Different letters indicate different levels of significance ($p < .05$) as determined by one-way ANOVA and Tukey's multiple comparisons test.

Our subsequent allelism test indicated that at least the steady-state alteration in NPQ and ΦPSII were unrelated to the loss of *NHD1* and of recessive genetic nature. The subsequent genome resequencing of pooled F_2 SALK_008491 individuals reproducing the original phenotype uncovered a homozygous 14-kb deletion on Chr3 just upstream of the *NHD1* locus. Our follow-up studies with independent lines and F_1 crosses confirmed that increased steady-state NPQ is caused by the absence of *PGDH3* the adjacent locus to *NHD1*. PGDH3 converts 3-phosphoglycerate into serine precursors yielding NADH. This short reaction pathway seems to avoid PSI acceptor side limitations through providing an alternative electron sink to reoxidize the stromal NADP pool (Hohner et al., 2021; Kramer & Kunz, 2021).

Interestingly, DEPI monitoring revealed that although SALK_008491 plants shared traits with two independent *pgdh3* loss-of-function alleles, it generally behaved more extreme when exposed to sigmoidal high light and sigmoidal dynamic light (e.g., NPQ, loss of biomass, and increased qE sensitivity at lower LEF). Indeed, in long-term dynamic growth light experiments, SALK_008491 plants exhibited drastically diminished growth and severe photodamaged characterized by low F_v/F_m and ΦPSII. Through the study of single mutants and genetic complementation, we showed that the extreme response to dynamic light is due to collective loss of both plastid proteins, PGDH3 and NHD1. We also found that the loss of NHD1 alone results in dynamic light-susceptible mutant plants, albeit to a less severe extent. We hope this finding encourages further studies into the relevance of NHD1 to the plant's acclimation potential. NHD1 was initially described as a plastid envelope Na^+/H^+ exchanger (Furumoto et al., 2011). Later, it was detected in stroma lamellae fractions from isolated Arabidopsis thylakoid membranes through proteomics (Tomizioli et al., 2014). Therefore, a role in the regulation of the pmf cannot be ruled out at this point. Unfortunately, no suitable *nhd1* T-DNA insertions lines are available currently. The *nhd1-1* allele harbors the here described homozygous 14-kb deletion upstream of NHD1. The second available allele *nhd1-2* yields only viable heterozygous individuals probably due to an uncharacterized second-site mutation that causes homozygous lethality. Because of these genetic uncertainties and the unknown effect of heterozygous deletions and mutations, the here employed *nhd1-1nhd1-2* crossed allele serves as a temporary solution at best. CRISPR/Cas9 genome editing may yield side effect-free *nhd1* loss-of-function alleles.

Over the last years, the possibility of affordable mutant genome resequencing has provided unprecedented insights into the complex genome architecture that can emerge from T-DNA mutagenesis. Chromosome rearrangements as well as small indels have been discovered frequently (Jupe et al., 2019). In addition, larger deletions (31 insertions with deletions larger than 1000 bp, eight of them larger than 5 kb) were revealed by short-read sequencing in the GABI-Kat collection (Kleinboelting et al., 2015). One of these, a 6.1-kb deletion on Chr3, affected three genes in total, which caused a previously undescribed phenotype. In some cases, sequencing results that

appeared as genomic deletions were merely due to faulty TAIR9 genome assembly in specific chromosomal regions (Pucker et al., 2021). Based on our follow-up PCR genotyping, we can exclude a rearrangement or misannotation for the 14-kb deletion of interest on Chr3 in SALK_008491.

Large genomic deletions can be valuable research tools. For instance, a rare recombination event between T-DNAs from two single-insertion lines gave rise to 25-kb deletion on Chr4, eradicating three mitogen-activated protein (MAP) kinase kinases (MAPK1–3) loci, provided unique insights into the relevance of MAPKs (Su et al., 2013). Using CRISPR/Cas9 genome editing or argon irradiation, viable Arabidopsis mutants carrying 30- to 70-kb (Grutzner et al., 2021) and even 940-kb deletion respectively (Sanjaya et al., 2021) have been isolated. The growing number of transgenic lines with large genomic deletions upstream and downstream of the T-DNA insertion suggests more deletion lines at the stock centers likely exist. Low-coverage mutant genome resequencing (used here), protocols such as 4SEE (Krispil et al., 2020), or multiplexed RNA-SEQ combined with bioinformatic tools for alignments, pseudoalignments, and variant calling can be utilized to spot unknown T-DNA insertion sites (Bray et al., 2016; Inagaki et al., 2015; Lambirth et al., 2015; Park et al., 2017; Sun et al., 2019).

In the case of SALK_008491, we were able to describe a new phenotype, that is, severe sensitivity towards dynamic light treatments, which emerges from the loss of the two plastid proteins PGDH3 and NHD1. According to SUBA4 (Hooper et al., 2017), the other deleted four loci encode for proteins outside the chloroplast (Table 1). The loss of PGDH3 causes increase PSI acceptor side limitation as shown before (Hohner et al., 2021). We hypothesize that the additional loss of NHD1, which may also facilitate ion flux across the thylakoid membrane (Tomizioli et al., 2014), further affects the membrane potential component of the pmf, $\Delta\psi$. High $\Delta\psi$ results in severe charge recombination within PSII (Davis et al., 2016). The combinatory effects therefore rapidly deteriorate SALK_008491 plants' performance when shifted into fluctuating light. New research into the role of NHD1 is required to understand its hypothetical role in pmf dynamics. This study shows that large deletion mutants can be useful genetic tools allowing new and unintuitive phenotypic insights.

4 | CONCLUSIONS

In the here reported study, we were able to add another large deletion Arabidopsis mutant to the public mutant repository through characterization of the SALK_008491 line. We show that two missing plastid proteins, PGDH3 and NHD1, individually play a role in the plant acclimation to dynamic light. Their joint loss has dramatic consequences for photosynthesis and growth of SALK_008491 under dynamic light stress. Our results encourage further studies into understanding the physiological significance of the plastid putative Na^+/H^+ exchanger NHD1. Moreover, we argue for the importance to report large deletion Arabidopsis mutants as they can be used to gain unintuitive insights into complex genetic and physiological traits. A collection of Arabidopsis large deletion mutants may support efforts to define the minimal nuclear genome for the design synthetic plant cells.

5 | MATERIALS AND METHODS

5.1 | Growth conditions

A. thaliana WT and mutant plants (accession Columbia-0 [Col-0]) were germinated on one-half Murashige and Skoog (MS), 1% phytoagar plates pH 5.8 for 7 days in a growth chamber (CU-41L4; Percival Scientific) with 150 μmol photons m^{-2} s^{-1} of continuous light (cool-white fluorescent bulbs), 16/8-h light:dark cycle. After potting plants on soil (Sungro Professional Growing Mix #1, Sun Gro Horticulture, Agawam, MA, USA), they were shifted to self-built growth racks with 120 μmol photons m^{-2} s^{-1} of continuous light in 12/12-h light:dark cycles and room temperature 22°C (Schneider et al., 2019). When individuals were designated for light treatments, 2-week-old plants were moved either into constant high light (900 μmol photons m^{-2} s^{-1}) or into fluctuating light for 2 weeks. The SALK_008491 (*nhd1-1*) and Sail107_F07 aka *nhd1-2* were originally obtained from ABRC but used in an earlier study (Muller et al., 2014). The *nhd1-1nhd1-2* mutant line was generated by crossing of respective single mutants. Subsequent BASTA selection of progenies ensured that both insertions were maintained in a heterozygous state. As described previously, this results in an another viable overall homozygous *nhd1* loss-of-function allele (Muller et al., 2014).

5.2 | PCR-based genotyping

In all reactions, Phusion® High-Fidelity DNA Polymerase (New England Biolabs, Ipswich, MA, USA) was used. The standard thermocycler settings used were 96°C for 2 min, followed by 30 cycles of 94°C for 10 s, 55°C for 30 s, and 72°C for 30–60 s. Final elongation was at 72°C for 5 min. PCR products were visualized by agarose gel electrophoresis and ethidium bromide staining. The primers used to confirm the 14-kb genomic deletion by PCR can be found under Table S1.

5.3 | Chlorophyll *a* fluorescence measurements

A MAXI version IMAGING-PAM (IMAG-K7 by Walz, Effeltrich, Germany) was employed in all experiments in all photosynthesis-related experiments with the exception of DEPI runs. Before each measurement, plants were positioned in customized plant holders. Subsequently, plants were dark-adapted for 15 min followed by recording of a standard induction curve at 186-μmol photons m^{-2} s^{-1} actinic light (Kunz et al., 2009). Image extraction and data analysis were performed as described earlier (Schneider et al., 2019).

Homozygous loss-of-function lines were monitored by DEPI at the Center for Advanced Algal and Plant Phenotyping at Michigan

State University for five consecutive days using dynamic light intensities as described earlier (Cruz et al., 2016). DEPI results were calculated as described in Cruz et al. (2016). qE is also referred to as NPQ_f and qI as NPQ_s, respectively.

5.4 | Genome sequencing and assembly using Illumina reads

gDNA from SALK_008491 was extracted from leaf tissue using the NucleoSpin Plant II kit (MACHEREY-NAGEL, Düren, Germany). From the purified gDNA sample, plant and animal whole-genome library (350 bp) was prepared and sequenced on an Illumina NovaSeq 6000 with 150-bp paired ends and 4-GB output (Novogene, Beijing, China). The raw sequencing data from SALK_008491 can be found at PRJNA802985. Reads were obtained in fq format and aligned to the TAIR annotation release 10 of the *A. thaliana* reference genome in fasta format and with pROK2 plasmid sequence (CD3-445) added in as an extra chromosome. The following programs were used: Bowtie2 (Langmead & Salzberg, 2012), SAMtools (Li et al., 2009), and lumpy-sv (Layer et al., 2014). Genome alignments were visualized with the Integrative Genomics Viewer (Robinson et al., 2011). Col-0 WT reads for genome comparisons were taken from SRA accession ID: PRJNA590836 (David et al., 2019).

5.5 | Automated phenotyping

SALK_008491 T-DNA line and corresponding WT plants were imaged for 22 days inside WSU's Compact Plants Phenomics Center (LemnaTech, Aachen, Germany) (Li et al., 2021). Constant light treatment was 100 μmol photons m^{-2} s^{-1} in a 12-h light/12-h dark cycle at 22°C/18°C, and fluctuating light treatment was 1 min at 500 μmol photons m^{-2} s^{-1} and 4 min at 100 μmol photons m^{-2} s^{-1} in a 12-h light/12-h dark cycle at 22°C/18°C. RGB picture and chlorophyll *a* fluorescence data were acquired on a daily basis.

5.6 | Generation of SALK_008491 pG20_Hyg::PGDH3-mCherry and TAC complementation lines

The pG20_Hyg::PGDH3-mCherry construct was generated by amplifying PGDH3 cDNA (sense primer: cgcgccactagtggatccatggcgacgtctctgaatctatc/antisense primer: cccttgctcaccatcccgggtagtttgaggaaaacaaactcttcaatggcagg) without stop codon from a total leaf cDNA pool. The resulting product was inserted into a BamHI/XmaI cut pG20_mCherry_Hyg vector by Gibson cloning (Pratt et al., 2020). The TAC clones K19N23 and K25N10 were ordered from ABRC. The constructs were transformed into SALK_008491 by floral dip (Clough & Bent, 1998). Individual transgenic plants were initially selected on the basis of resistance to hygromycin, respectively. The presence of the constructs was confirmed by PCR. Furthermore, the construct presence in SALK_008491 + *pUBQ10:PGDH3::mCherry* was confirmed on a Leica SP5 confocal microscope. mCherry excitation occurred at 587 nm, and emission at 594–671 nm was detected. Lastly, the degreed of PGDH3 overexpression was measured using total PGDH activity assay (Hohner et al., 2021).

5.7 | Immunoblotting of PGDHs and NHD1

Immunoblotting of total PGDH protein in leaf extracts was done exactly as described earlier (Hohner et al., 2021). To allow for NHD1 detection, an α-NHD1 immunoglobulin was commercially generated (YenZym Antibodies, San Francisco, CA, USA). As an antigen, a short peptide corresponding to the N-terminal loop in NHD1 was synthesized (AAs:#95∼113: VDEPSSSYFEANYQPKTDI). The resulting α-NHD1 gave only weak NHD1 signal in total leaf extracts and was therefore detected using SuperSignal West Femto ECL Substrate (Thermo Scientific™).

ACCESSION NUMBERS

NHD1 (At3g19490), *PGDH3* (At3g19480), SALK_008491 (CS72464) aka *nhd1-1* (Muller et al., 2014), *nhd1-1nhd1-2* (Sail107_F07) (Muller et al., 2014), *pgdh3-1* mutant (SM_3_37584, CS72462) (Toujani et al., 2013), *pgdh3-2* (GK-877F12, CS72463) (Toujani et al., 2013), TAC K19N23 (Liu et al., 1999), and TAC K25N10 (Liu et al., 1999).

ACKNOWLEDGMENTS

We thank David Hall and Dr. Sebastian Kuhlgert (Michigan State University) for support with DEPI experiments. Undergraduate research by C. M. L. and C. L. L. at Washington State University (WSU) was financially supported through the School of Biological Sciences, the College of Arts and Sciences, the WSU undergraduate research office, and the NASA Space Grant Fellowship. L. S. S., C. M. L., and C. L. L. thank the DAAD RISE Germany program for their science abroad experience. Open Access funding enabled and organized by Projekt DEAL. WOA Institution: LUDWIG-MAXIMILIANS-UNIVERSITAET MUNCHEN Consortia Name : Projekt DEAL

CONFLICTS OF INTEREST

The authors declare no conflicts of interest.

AUTHOR CONTRIBUTIONS

H.-H. K. designed the research, cloned the constructs, isolated the plant mutants, performed the initial experiments, analyzed the data, and wrote the manuscript. L. S. L. performed the plant phenotyping, deep sequencing, and genetic mapping, analyzed the data, cloned the constructs, and isolated the mutants with the assistance of C. M. L. and C. L. L. C. V. analyzed the data, prepared the figures, and assisted in the writing of the manuscript. P. M. D. carried out the immunoblotting and PGDH activity assays. D. S. performed the plant phenotyping and analyzed the data. V. C. G. and U. A. replicated the fluctuating light response studies in an independent institution and analyzed the data. J. A. C. and D. M. K. performed and analyzed the

dynamic environmental photosynthetic imaging. All the authors assisted in editing the manuscript.

ORCID

Laura S. Lopez https://orcid.org/0000-0003-4038-9199
Carsten Völkner https://orcid.org/0000-0001-8196-0828
Philip M. Day https://orcid.org/0000-0002-9030-0511
Dominik Schneider https://orcid.org/0000-0002-5846-5033
Viviana Correa Galvis https://orcid.org/0000-0002-8092-9148
Jeffrey A. Cruz https://orcid.org/0000-0003-1098-5176
Ute Armbruster https://orcid.org/0000-0002-8814-8207
David M. Kramer https://orcid.org/0000-0003-2181-6888
Hans-Henning Kunz https://orcid.org/0000-0001-8000-0817

REFERENCES

Armbruster, U., Correa Galvis, V., Kunz, H.-H., & Strand, D. D. (2017). The regulation of the chloroplast proton motive force plays a key role for photosynthesis in fluctuating light. *Current Opinion in Plant Biology*, *37*, 56–62. https://doi.org/10.1016/j.pbi.2017.03.012

Benstein, R. M., Ludewig, K., Wulfert, S., Wittek, S., Gigolashvili, T., Frerigmann, H., Gierth, M., Flugge, U. I., & Krueger, S. (2013). *Arabidopsis* phosphoglycerate dehydrogenase1 of the phosphoserine pathway is essential for development and required for ammonium assimilation and tryptophan biosynthesis. *Plant Cell*, *25*(12), 5011–5029. https://doi.org/10.1105/tpc.113.118992

Bray, N. L., Pimentel, H., Melsted, P., & Pachter, L. (2016). Near-optimal probabilistic RNA-seq quantification. *Nature Biotechnology*, *34*, 525–527. https://doi.org/10.1038/nbt.3519

Casatejada-Anchel, R., Munoz-Bertomeu, J., Rosa-Tellez, S., Anoman, A. D., Nebauer, S. G., Torres-Moncho, A., Fernie, A. R., & Ros, R. (2021). Phosphoglycerate dehydrogenase genes differentially affect Arabidopsis metabolism and development. *Plant Science*, *306*, 110863. https://doi.org/10.1016/j.plantsci.2021.110863

Clough, S. J., & Bent, A. F. (1998). Floral dip: A simplified method for Agrobacterium-mediated transformation of Arabidopsis thaliana. *The Plant Journal : For Cell and Molecular Biology*, *16*(6), 735–743.

Cruz, J. A., Savage, L. J., Zegarac, R., Hall, C. C., Satoh-Cruz, M., Davis, G. A., Kovac, W. K., Chen, J., & Kramer, D. M. (2016). Dynamic environmental photosynthetic imaging reveals emergent phenotypes. *Cell Systems*, *2*(6), 365–377. https://doi.org/10.1016/j.cels.2016.06.001

Dash, L., McEwan, R. E., Montes, C., Mejia, L., Walley, J. W., Dilkes, B. P., & Kelley, D. R. (2021). *slim shady* is a novel allele of *PHYTOCHROME B* present in the T-DNA line SALK_015201. *Plant Direct*, *5*(6), e00326. https://doi.org/10.1002/pld3.326

David, R., Kortschak, R., & Searle, I. (2019). The root hair defective phenotype of *Arabidopsis thaliana* Pol IV subunit mutant *nrpd1a-3* is associated with a deletion in RHD6. *microPublication Biology*, *2019*.

Davis, G. A., Kanazawa, A., Schöttler, M. A., Kohzuma, K., Froehlich, J. E., Rutherford, A. W., Satoh-Cruz, M., Minhas, D., Tietz, S., Dhingra, A., & Kramer, D. M. (2016). Limitations to photosynthesis by proton motive force-induced photosystem II photodamage. *eLife*, *5*, e16921. https://doi.org/10.7554/eLife.16921

Furumoto, T., Yamaguchi, T., Ohshima-Ichie, Y., Nakamura, M., Tsuchida-Iwata, Y., Shimamura, M., Ohnishi, J., Hata, S., Gowik, U., Westhoff, P., Bräutigam, A., Weber, A. P. M., & Izui, K. (2011). A plastidial sodium-dependent pyruvate transporter. *Nature*, *476*(7361), 472–475. https://doi.org/10.1038/nature10250

Grutzner, R., Martin, P., Horn, C., Mortensen, S., Cram, E. J., Lee-Parsons, C. W. T., Stuttmann, J., & Marillonnet, S. (2021). High-efficiency genome editing in plants mediated by a Cas9 gene containing multiple introns. *Plant Communications*, *2*, 100135. https://doi.org/10.1016/j.xplc.2020.100135

Hohner, R., Day, P. M., Zimmermann, S. E., Lopez, L. S., Kramer, M., Giavalisco, P., Correa Galvis, V., Armbruster, U., Schottler, M. A., Jahns, P., Krueger, S., & Kunz, H. H. (2021). Stromal NADH supplied by PHOSPHOGLYCERATE DEHYDROGENASE3 is crucial for photosynthetic performance. *Plant Physiology*, *186*, 142–167. https://doi.org/10.1093/plphys/kiaa117

Höhner, R., Galvis, V. C., Strand, D. D., Völkner, C., Krämer, M., Messer, M., Dinc, F., Sjuts, I., Bölter, B., Kramer, D. M., Armbruster, U., & Kunz, H.-H. (2019). Photosynthesis in Arabidopsis is unaffected by the function of the vacuolar K^+ channel TPK3. *Plant Physiology*, *180*(3), 1322–1335. https://doi.org/10.1104/pp.19.00255

Holzwarth, A. R., Lenk, D., & Jahns, P. (2013). On the analysis of non-photochemical chlorophyll fluorescence quenching curves: I. Theoretical considerations. *Biochimica et Biophysica Acta*, *1827*(6), 786–792. https://doi.org/10.1016/j.bbabio.2013.02.011

Hooper, C. M., Castleden, I. R., Tanz, S. K., Aryamanesh, N., & Millar, A. H. (2017). SUBA4: The interactive data analysis centre for Arabidopsis subcellular protein locations. *Nucleic Acids Research*, *45*, D1064–D1074. https://doi.org/10.1093/nar/gkw1041

Inagaki, S., Henry, I. M., Lieberman, M. C., & Comai, L. (2015). High-throughput analysis of T-DNA location and structure using sequence capture. *PLoS ONE*, *10*, e0139672. https://doi.org/10.1371/journal.pone.0139672

Johnson, M., & Ruban, A. (2013). Rethinking the existence of a steady-state $\Delta\psi$ component of the proton motive force across plant thylakoid membranes. *Photosynthesis Research*, *119*, 233–242.

Jupe, F., Rivkin, A. C., Michael, T. P., Zander, M., Motley, S. T., Sandoval, J. P., Slotkin, R. K., Chen, H., Castanon, R., Nery, J. R., & Ecker, J. R. (2019). The complex architecture and epigenomic impact of plant T-DNA insertions. *PLoS Genetics*, *15*, e1007819. https://doi.org/10.1371/journal.pgen.1007819

Kanazawa, A., & Kramer, D. M. (2002). *In vivo* modulation of nonphotochemical exciton quenching (NPQ) by regulation of the chloroplast ATP synthase. *Proceedings of the National Academy of Sciences of the United States of America*, *99*, 12789–12794. https://doi.org/10.1073/pnas.182427499

Kleinboelting, N., Huep, G., Appelhagen, I., Viehoever, P., Li, Y., & Weisshaar, B. (2015). The structural features of thousands of T-DNA insertion sites are consistent with a double-strand break repair-based insertion mechanism. *Molecular Plant*, *8*(11), 1651–1664. https://doi.org/10.1016/j.molp.2015.08.011

Kleine, T., Nagele, T., Neuhaus, H. E., Schmitz-Linneweber, C., Fernie, A. R., Geigenberger, P., Grimm, B., Kaufmann, K., Klipp, E., Meurer, J., Mohlmann, T., Muhlhaus, T., Naranjo, B., Nickelsen, J., Richter, A., Ruwe, H., Schroda, M., Schwenkert, S., Trentmann, O., … Leister, D. (2021). Acclimation in plants—the Green Hub consortium. *The Plant Journal*, *106*, 23–40. https://doi.org/10.1111/tpj.15144

Kramer, M., & Kunz, H. H. (2021). Indirect export of reducing equivalents from the chloroplast to resupply NADP for C_3 photosynthesis-growing importance for stromal NAD(H)? *Frontiers in Plant Science*, *12*, 719003. https://doi.org/10.3389/fpls.2021.719003

Krispil, R., Tannenbaum, M., Sarusi-Portuguez, A., Loza, O., Raskina, O., & Hakim, O. (2020). The position and complex genomic architecture of plant T-DNA insertions revealed by 4SEE. *International Journal of Molecular Sciences*, *21*(7), 2373. https://doi.org/10.3390/ijms21072373

Kunz, H.-H., Scharnewski, M., Feussner, K., Feussner, I., Flügge, U.-I., Fulda, M., & Gierth, M. (2009). The ABC transporter PXA1 and peroxisomal β-oxidation are vital for metabolism in mature leaves of

Arabidopsis during extended darkness. *The Plant Cell*, *21*(9), 2733–2749. https://doi.org/10.1105/tpc.108.064857

Lambirth, K. C., Whaley, A. M., Schlueter, J. A., Bost, K. L., & Piller, K. J. (2015). CONTRAILS: A tool for rapid identification of transgene integration sites in complex, repetitive genomes using low-coverage paired-end sequencing. *Genomics Data*, *6*, 175–181. https://doi.org/10.1016/j.gdata.2015.09.001

Langmead, B., & Salzberg, S. L. (2012). Fast gapped-read alignment with Bowtie 2. *Nature Methods*, *9*(4), 357–359. https://doi.org/10.1038/nmeth.1923

Layer, R. M., Chiang, C., Quinlan, A. R., & Hall, I. M. (2014). LUMPY: A probabilistic framework for structural variant discovery. *Genome Biology*, *15*(6), R84. https://doi.org/10.1186/gb-2014-15-6-r84

Li, H., Handsaker, B., Wysoker, A., Fennell, T., Ruan, J., Homer, N., Marth, G., Abecasis, G., Durbin, R., & 1000 Genome Project Data Processing Subgroup. (2009). The sequence alignment/map format and SAMtools. *Bioinformatics*, *25*(16), 2078–2079. https://doi.org/10.1093/bioinformatics/btp352

Li, M., Svoboda, V., Davis, G., Kramer, D., Kunz, H. H., & Kirchhoff, H. (2021). Impact of ion fluxes across thylakoid membranes on photosynthetic electron transport and photoprotection. *Nature Plants*, *7*, 979–988. https://doi.org/10.1038/s41477-021-00947-5

Liu, Y. G., Shirano, Y., Fukaki, H., Yanai, Y., Tasaka, M., Tabata, S., & Shibata, D. (1999). Complementation of plant mutants with large genomic DNA fragments by a transformation-competent artificial chromosome vector accelerates positional cloning. *Proceedings of the National Academy of Sciences of the United States of America*, *96*(11), 6535–6540. https://doi.org/10.1073/pnas.96.11.6535

Muller, M., Kunz, H. H., Schroeder, J. I., Kemp, G., Young, H. S., & Neuhaus, H. E. (2014). Decreased capacity for sodium export out of Arabidopsis chloroplasts impairs salt tolerance, photosynthesis and plant performance. *The Plant Journal*, *78*(4), 646–658. https://doi.org/10.1111/tpj.12501

OMalley, R. C., Barragan, C. C., & Ecker, J. R. (2015). A user's guide to the Arabidopsis T-DNA insertion mutant collections. In J. M. Alonso & A. N. Stepanova (Eds.), *Plant functional genomics: Methods and protocols* (Vol. 1284) (pp. 323–342). Springer New York. https://doi.org/10.1007/978-1-4939-2444-8_16

Park, D., Park, S. H., Ban, Y. W., Kim, Y. S., Park, K. C., Kim, N. S., Kim, J. K., & Choi, I. Y. (2017). A bioinformatics approach for identifying transgene insertion sites using whole genome sequencing data. *BMC Biotechnology*, *17*, 67. https://doi.org/10.1186/s12896-017-0386-x

Pratt, A. I., Knoblauch, J., & Kunz, H. H. (2020). An updated pGREEN-based vector suite for cost-effective cloning in plant molecular biology. *microPublication Biology*, *2020*.

Pucker, B., Kleinbolting, N., & Weisshaar, B. (2021). Large scale genomic rearrangements in selected *Arabidopsis thaliana* T-DNA lines are caused by T-DNA insertion mutagenesis. *BMC Genomics*, *22*(1), 599. https://doi.org/10.1186/s12864-021-07877-8

Robinson, J. T., Thorvaldsdottir, H., Winckler, W., Guttman, M., Lander, E. S., Getz, G., & Mesirov, J. P. (2011). Integrative genomics viewer. *Nature Biotechnology*, *29*(1), 24–26. https://doi.org/10.1038/nbt.1754

Sanjaya, A., Kazama, Y., Ishii, K., Muramatsu, R., Kanamaru, K., Ohbu, S., Abe, T., & Fujiwara, M. T. (2021). An argon-ion-induced pale green mutant of *Arabidopsis* exhibiting rapid disassembly of mesophyll chloroplast grana. *Plants (Basel)*, *10*(5), 848. https://doi.org/10.3390/plants10050848

Schneider, D., Lopez, L. S., Li, M., Crawford, J. D., Kirchhoff, H., & Kunz, H. H. (2019). Fluctuating light experiments and semi-automated plant phenotyping enabled by self-built growth racks and simple upgrades to the IMAGING-PAM. *Plant Methods*, *15*, 156. https://doi.org/10.1186/s13007-019-0546-1

Strand D. D., Kramer D. M. (2014). Control of non-photochemical exciton quenching by the proton circuit of photosynthesis. *In* B. Demmig-Adams, G. Garab, W. Adams III, & Govindjee, (Eds.), *Non-photochemical quenching and energy dissipation in plants, algae and cyanobacteria* (Vol. 40, pp. 387–408). Springer Netherlands. https://doi.org/10.1007/978-94-017-9032-1_18

Su, S. H., Bush, S. M., Zaman, N., Stecker, K., Sussman, M. R., & Krysan, P. (2013). Deletion of a tandem gene family in *Arabidopsis*: Increased MEKK2 abundance triggers autoimmunity when the MEKK1-MKK1/2-MPK4 signaling cascade is disrupted. *Plant Cell*, *25*(5), 1895–1910. https://doi.org/10.1105/tpc.113.112102

Sun, L., Ge, Y., Sparks, J. A., Robinson, Z. T., Cheng, X., Wen, J., & Blancaflor, E. B. (2019). TDNAscan: A software to identify complete and truncated T-DNA insertions. *Frontiers in Genetics*, *10*, 685. https://doi.org/10.3389/fgene.2019.00685

Tomizioli, M., Lazar, C., Brugiere, S., Burger, T., Salvi, D., Gatto, L., Moyet, L., Breckels, L. M., Hesse, A.-M., Lilley, K. S., Seigneurin-Berny, D., Finazzi, G., Rolland, N., & Ferro, M. (2014). Deciphering thylakoid sub-compartments using a mass spectrometry-based approach. *Molecular & Cellular Proteomics*, *13*(8), 2147–2167. https://doi.org/10.1074/mcp.M114.040923

Toujani, W., Munoz-Bertomeu, J., Flores-Tornero, M., Rosa-Tellez, S., Anoman, A. D., Alseekh, S., Fernie, A. R., & Ros, R. (2013). Functional characterization of the plastidial 3-phosphoglycerate dehydrogenase family in Arabidopsis. *Plant Physiology*, *163*, 1164–1178. https://doi.org/10.1104/pp.113.226720

SUPPORTING INFORMATION

Additional supporting information can be found online in the Supporting Information section at the end of this article.

How to cite this article: Lopez, L. S., Völkner, C., Day, P. M., Lewis, C. M., Lewis, C. L., Schneider, D., Correa Galvis, V., Cruz, J. A., Armbruster, U., Kramer, D. M., & Kunz, H.-H. (2022). The Arabidopsis T-DNA mutant SALK_008491 carries a 14-kb deletion on chromosome 3 that provides rare insights into the plant response to dynamic light stress. *Plant Direct*, *6*(7), e429. https://doi.org/10.1002/pld3.429